Applied Physics B (2019) 125:225
https://doi.org/10.1007/s00340-019-7334-5

Applied Physics B
Lasers and Optics

Ultrafast modification of oxide glass surface hardness

Sean Locker[1] · **S. K. Sundaram**[1]

Received: 28 January 2019 / Accepted: 20 October 2019 / Published online: 6 November 2019

Abstract
Application of femtosecond lasers is widely utilized in micromachining transparent materials. We have successfully altered the surface hardness of various commercial silicate glasses using a high-intensity femtosecond pulse laser. The femtosecond laser generates pulse energy of 500 nJ with a central wavelength of 800 nm. Using a peak power of 2.2 W and a repetition rate of 5.1 MHz, we observed an 18–20% increase surface hardness in glasses with low-modifier content and 16.6% decrease in glasses with high-modifier content. All laser exposed glasses show no detectable induced-crystallization or surface ablation. X-ray photoelectron spectroscopy results of our samples confirmed that the laser irradiation had no detectable effect on surface chemistry. X-ray reflectometry data showed the change in hardness was attributed to a thin layer with modified density. Experimental results suggest the strengthening mechanism derives from local structural transformation of interatomic bond distances and angles.

1 Introduction

The interaction between femtosecond laser pulses and transparent materials has become an actively researched topic over the past two decades [1–3]. Recently, many interesting phenomena induced by femtosecond laser irradiation in transparent materials have been reported, i.e., nonreciprocity writing, oxidation and reduction of dopants, migration of ions and micro-fabrication of 3D structures [3–6]. Femtosecond laser pulses have the unique capability of irradiating a localized area with a large amount of energy. Deposition of energy in the glass network enables the structure to relax into a quasi-equilibrated state [7]. Controlling and optimizing the glass structure with laser pulses involve nonlinear absorption effects. Linear absorption is not observed in pure transparent materials because of insufficient photon energy needed to overcome the large bandgap; however, when sufficient energy is applied to a glass, significant nonlinear absorption takes place [1].

Classification of refractive index modification has been ascribed as type I and II. Regions with highly localized increases in refractive index relative to the unexposed bulk are known as type I. These changes are typically observed in laser exposures of low fluence and often result from local heating or melting followed by immediate cooling and the formation of color centers due to breaking Si–O bonds [8, 9]. Restructuring the glass matrix through a thermal process causes bond softening and subsequent ionic rearrangement; however, the degree of modulation is highly dependent on the thermal history and initial glass relaxation [10]. Type II refractive index changes are induced by high temperature and pressure gradients, resulting in the formation of stress fields [11].

Random network and space groups in glass provide an opportunity to distort bonds and interbonding angles. Applying intense femtosecond laser pulses to glass will produce a highly nonlinear interaction often resulting in permanent changes in material structure. Given the size of the incident beam, effective nonlinear interaction and subsequent modifications occur locally. Refractive index modifications via femtosecond laser irradiation have been observed with pulse energies ranging from 0.1 to 10 μJ and repetition rates from 1 to 100 kHz [12, 13]. These localized changes are highly dependent on composition and the positive or negative index changes tend to vary based on laser parameters. Processes using repetition rates greater than 200 kHz tend to observe minimal defect-induced damage [14]. The present paper provides methods to increase surface hardness by applying high repetition rate ultrafast laser pulses.

✉ Sean Locker
stl4@alfred.edu

[1] Ultrafast Materials Science and Engineering Laboratory (U-Lab), Kazuo Inamori School of Engineering, The New York State College of Ceramics, Alfred University, Alfred, NY, USA

Surface swelling is a common side effect observed during waveguide writing; laser-induced stresses manifest from confined quenching after near-surface exposure. Multiphoton absorption and subsequent plasma formation generate the necessary temperature and pressure to result in structural changes [15–17]. Localized energy deposited beneath the material surface mitigates material oblation, therefore, allowing stresses to develop as the irradiated region expands. As Bhardwaj et al. [17] outline, focusing just beneath the surface restricts lateral expansion and forcing expansion parallel to the incident beam, resulting in swelling. Another technique that results in increased hardness involves high-repetition laser pulses to redistribute ions into unique structures with enhanced properties. Ion migration is of interest because optical mechanical properties are related to elemental distribution. High-repetition rate femtosecond laser irradiation provides an opportunity to not only manipulate ionic positions, but also be spatially selective. Repetition rate is a crucial variable to ion migration as it proportionally effects localized heat accumulation. High-repetition rates accumulate significant heat, enabling bond-breaking and ion migration. Thermal diffusion within the focal point causes a temperature gradient, therefore elements with high diffusion coefficients escape to regions of lower temperature [1, 18, 19]. Vacancies within the laser-treated region are then occupied by network formers because the binding energy of former to oxygen is greater than former to modifier. This results in a more structured network with superior hardness. Finally, high-repetition laser pulses of low-intensity can create an environment in which structural rearrangement occurs without a redistribution of elements. Heat accumulation within the laser-focused region enables local changes to bond lengths and angles. However, before a thermal equilibration is reached, the structure is quenched. Observed structure relaxation is a result of transient laser-induced plasma generation and subsequent shock wave [20]. Highly focused beams are able to structurally alter a region under 1 μm [21]. Glass composition and modifier content play a large role in the laser-modified network; low modifier content shows change in Si–O network, high-modifier content observes primary variation to non-bridging oxygen (NBO) sites [20]. Unique laser energy regimes result in various modifications to the glass structure: densification, decompaction, and ablation. We present our results and interpretations on selected commercial glasses in this paper [22, 23].

2 Materials and methods

2.1 Femtosecond laser treatment and terahertz time domain spectroscopy analysis

We used a commercial femtosecond laser system, FEMTOLASER Scientific XL 500 (FEMTOLASERS Produktions GmbH, Austria) for our laser treatment. The solid-state Ti:Sapphire-based high energy oscillator system provides a pulse energy of 490 nJ, pulse duration of less than 50 fs, and a repetition rate of 5.1 MHz. The XL 500 system has four major components: pump source that continuously emits green light of 532 nm, a Ti:Sapphire oscillator chamber, a laser cavity including a multi-pass Herriot cell and a prism compressor to compress the pulses into femtosecond timescale. A plano-convex lens was used to focus the collimated beam, producing a Gaussian profile of $1/e^2$ beam radius 7.5 μm measured at the sample surface. Calculated peak exposure fluences of 1.59 J/cm^2 were derived from pulse energy measurements outlined by Liu [24]. Irradiation experiments were performed on polished surfaces held at a normal incidence to the laser beam and directed to the sample fixed to a XYZ translation stage (Thorlabs, USA). The mechanical translation stage was positioned for the focal point along the surface; this was done by maximizing fluorescence of the incident beam using a visualization system (CCD camera). The stage was moved in a two-dimensional plane normal to the beam. The sample was then rastered so parallel laser lines, 15 μm distant apart, were written across an area of 10 mm^2 at a speed of 2.2 mm/s. Figure 1 shows a schematic of our setup and rastering of a sample.

Soda-lime silicate (SLS), Borofloat (BF), and aluminoborosilicate (ABS) refractive indices were characterized using terahertz time domain spectroscopy (THz-TDS, TPS Spectra 3000, Teraview, UK). Terahertz radiation is produced by a mode-locked Ti:Sapphire laser with central wavelength of 800 nm, 80 MHz repetition rate and pulse width of 100 fs. The pulse is separated into a pump and probe beam; pump beam generates THz radiation and probe beam detects THz pulses using GaAs semiconductors. Samples were mounted on a holder with an optical aperture of 4.55 mm. Reference measurements were made with the empty sample holder in air. Broadband THz pulses are converted to a frequency regime through Fourier transformation. Measurements were performed by averaging 3000 scans with a resolution of 1.200 cm^{-1} and scan frequency of 30 Hz.

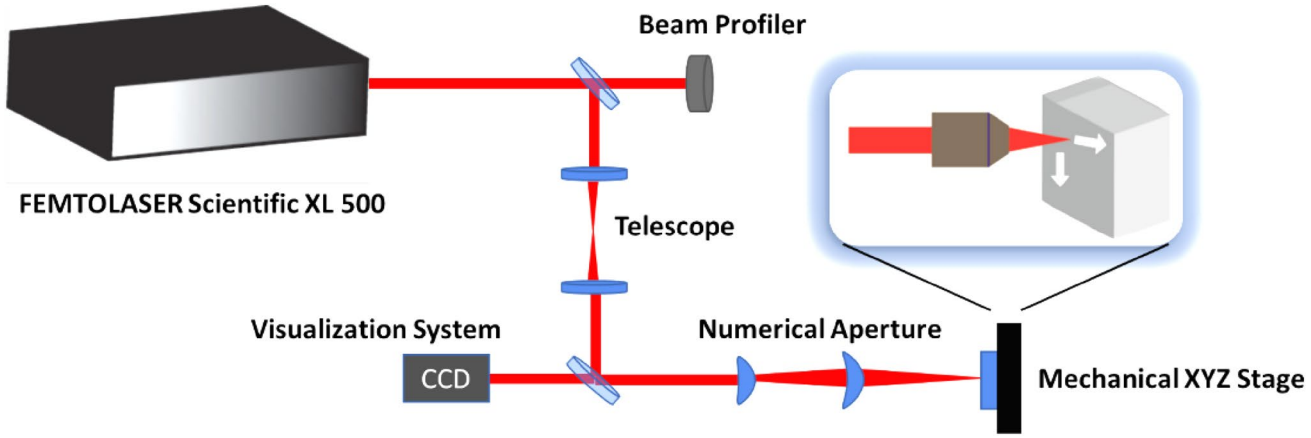

Fig. 1 Femtosecond laser irradiation setup and beam rastering module

2.2 X-ray photoelectron spectroscopy

All samples were cleaned with chemical detergent at room temperature, while immersed in an ultrasonic bath for 15 min. Nitrogen gas was used to dry samples before being stored in a vacuum desiccator. Prior to entering the introduction chamber, samples were placed into the ultraviolet ozone cleaner (UVOC) for 15 min to remove carbon and other atmospheric elements deposited on the surface. Survey scans were collected for qualitative analysis of elemental composition. High-resolution scans of each identified element were collected using the same pass energy and dwell time. Elemental identification and concentration were determined using both CasaXPS and MultiPak 8.0 software. Relative sensitivity factors were then used to normalize area under the curve and calculate quantitative elemental compositions for each glass. All elemental concentrations come with a plus or minus 1 at% error.

2.3 Surface hardness analysis

A series of indentations were made on laser-irradiated and non-irradiated regions of aluminosilicate, Borofloat and soda-lime glass. Micro-indentations were made with a pointed indenter on a Buehler Micromet II micro-hardness indenter. Surface hardness was calculated using Vickers hardness:

$$H_{\mathrm{V}} = 1.854\frac{F}{d^2}, \tag{1}$$

where F is the incident force measure in grams and d is the indentation diameter or cross section. Indentations were collected using 200 and 300 g of force and a 15 s loading time, under ambient conditions. After indentation, each of the diagonal lengths in the square-shaped indentation was measured on an American Optical Microscope at 100×.

2.4 X-ray reflectometry

X-ray reflectance (XRR) is a unique analysis technique well suited for determining the near-surface density (2–100 nm). Measurement was collected on a Bruker D8 Advanced X-ray Reflectometer using wavelength of 154 nm from 0.000° to 3.500° 2θ with a step size of 0.005°. DIFFRACT.XRR software was used to analyze XRR measurements through fitting a model against the measured data. Nevot-Croce roughness correction factor was used to define the vertical interface roughness and fit using a simulated annealing function.

3 Results and discussion

3.1 XPS analysis of glass surface chemistry

All X-ray photoelectron spectroscopy (XPS) survey scans revealed expected elemental composition on the surface. Peak identification was consistent with the bulk chemical analysis. High-resolution scans were collected for quantification of elemental composition. Elemental composition of manufacturer supplied glasses both before and after laser irradiation is found in Table 1. All composition showed a minimal change in Na ion concentration. Increased sodium concentration in SLS may be a result of the data collection and analysis; boundary position and band integration to determine composition. Minimal decrease in surface sodium content is likely a result of volatilization [25, 26]. In this case, observed sodium concentration falls within detectable error. Figure 2 compares elemental concentration before and after laser treatment; a—Na2s at 63 eV and Al2p at 73.6 eV, b—C1s at 284.2 eV and K2p ($K2p_{1/2}$ at 292.6 eV and $K2p_{3/2}$ at 295.6 eV), c—Ca2p ($Ca2p_{1/2}$ at 350.6 eV and $Ca2p_{3/2}$ at 347.0 eV), d—O1s at 531.6 eV, e—Si2p at 102.4 eV, and f—$Sn3d_{5/2}$ at 486.4 eV.

Table 1 Quantified silicate glass surface chemistry before and after laser irradiation

Glass/treatment	B	O	Na	Mg	Al	Si	K	Ca	Sn
ABS/untreated	2.8	65.5	1.5	1.3	1.0	25.8	1.3	0.2	0.6
ABS/treated	2.4	67.1	1.1	0.3	0.8	26.2	1.1	0.4	0.6
SLS/untreated	0.0	66.4	2.5	1.6	0.7	24.6	1.1	1.8	1.3
SLS/treated	0.0	66.3	3.0	0.9	0.5	25.3	1.2	1.6	1.2
BF/untreated	3.0	66.1	0.7	0.0	0.8	28.9	0.4	0.0	0.1
BF/treated	2.7	67.5	0.6	0.0	0.7	28.0	0.3	0.0	0.1

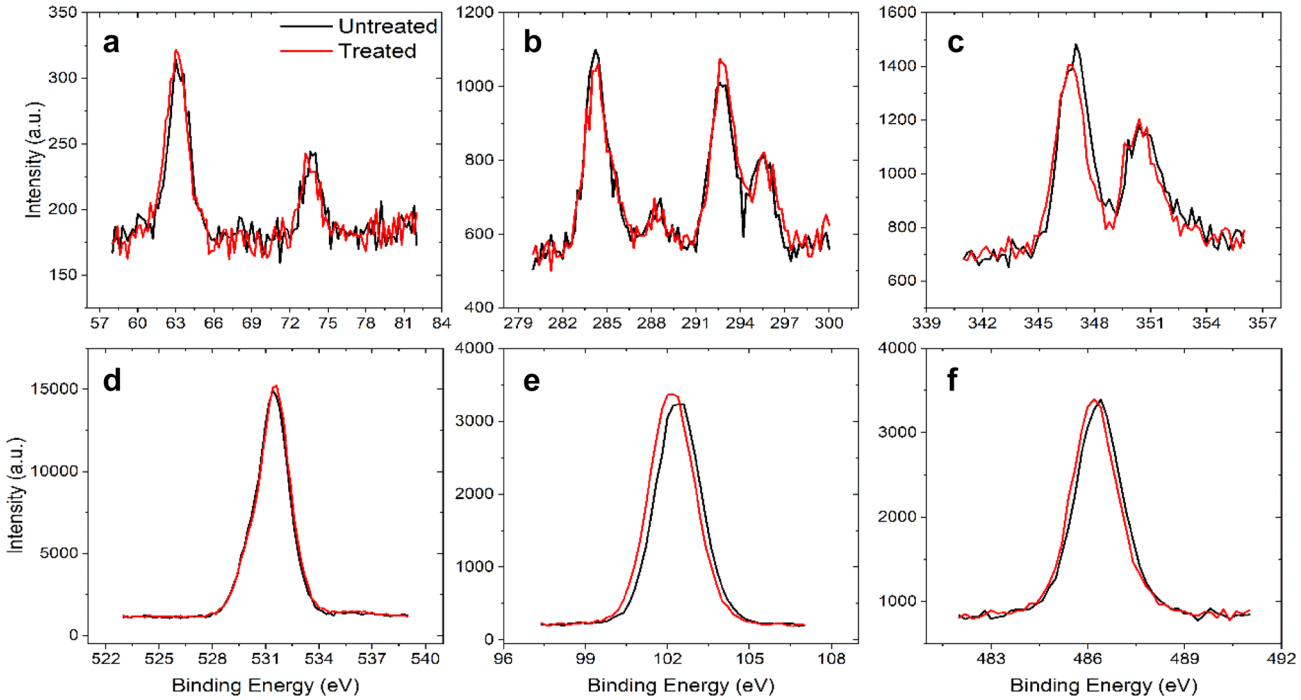

Fig. 2 High-resolution XPS scans of SLS glass before (black) and after (red) laser irradiation

In laser-irradiated ABS glass, we observed a depletion of $\leq 0.4\%$ and a surface enrichment in oxygen and silicon of $\leq 1.1\%$ and 0.4%, respectively. The minimal depletion of boron, sodium, and aluminum is within the measurable associated error and standard deviation of 0.5 at%. However, thermal effects have been documented to induce the depletion of the previous elements in the literature [27].

Similar depletions were observed in both SLS and Borofloat glasses. Surface analysis showed minimal depletion of Mg $\leq 0.8\%$ in SLS. Loss of magnesium in both SLS and ABS glasses can be a thermal effect; however, the depletion or enrichment of a cation species less than 1.5% is hard to definitively attribute to the femtosecond laser. The enrichment of sodium along the SLS glass surface lies within the measurable standard deviation and shows no conclusive evidence of ion migration in any other cation species.

Laser-induced effects in BF glass were expected to be significantly different because of the low modifier content and lack of alkaline earth ions. BF ionic content within laser-irradiated region, seen in Fig. 3, shows no significant change after high-intensity pulse exposure. Elements shown in Fig. 3 are as follows: a—Na1s and Al2p, b—B1s at 192.2 eV, c—C1s, d—O1s, e—Si2p, and f—$Sn3d_{5/2}$. Small amounts of potassium are found in Fig. 3c at 293 eV. Post-exposure high-resolution scans are nearly identical to the pristine sample, aside from the minimal shift of Si2p observed in both SLS and BF glass.

ABS high-resolution scans are shown in Fig. 4. Similar to SLS and BF, laser exposure has no observable effect on ion concentration at the glass surface. XPS scans of the detectable elements in ABS glass include a—Al2p, b—B1s, c—C1s, $K2p_{1/2}$, and $K2p_{3/2}$, d—Ca2p, e—O1s, and f—Si2p. The symmetric O1 s peak indicates that the bridging oxygen (BO) to non-bridging oxygen (NBO) ratio is unaffected by laser irradiation; therefore, proving femtosecond laser pulses do not cause restructuring in the glass network.

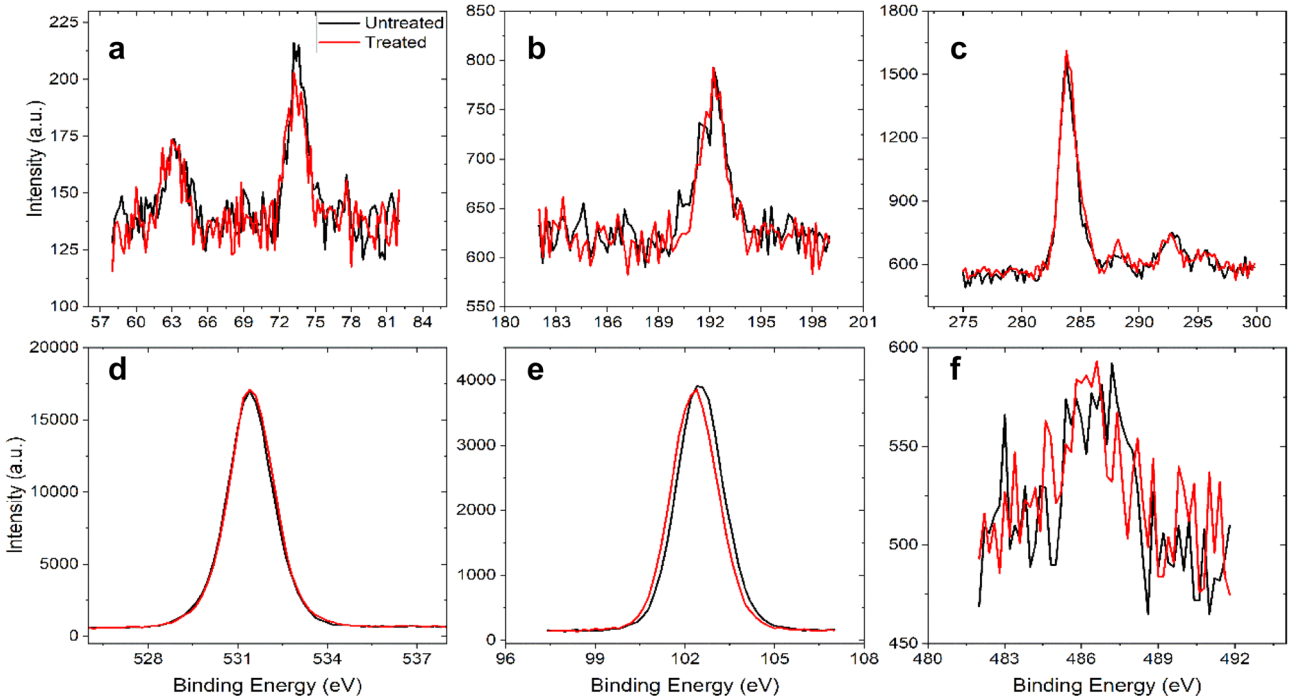

Fig. 3 High-resolution XPS scans of BF glass before (dash) and after (dot) laser irradiation

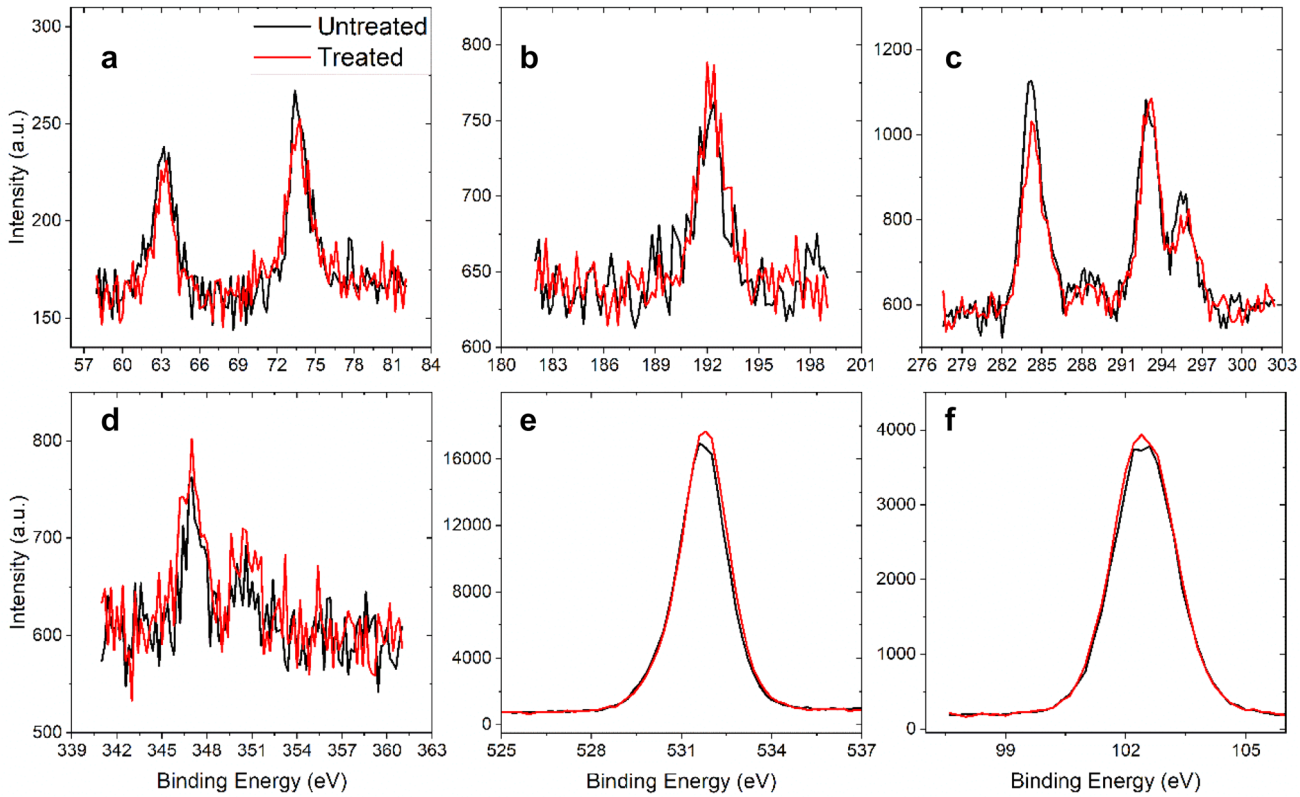

Fig. 4 High-resolution XPS scans of ABS glass before (dash) and after (dot) laser irradiation

Ion concentration along the glass surface is of interest because of the thermal and optical affects induced by the femtosecond laser (i.e., ion migration of network modifying agents that may induce surface stress layers). It has been shown that high-intensity laser pulses cause minimal change to glass surface chemistry. Unlike Luo et al. [18] and Shimizu et al. [19], where elemental distribution was observed under high-repetition-rate femtosecond laser exposure with peak fluences of 10.7 and 63.8 J/cm^2, respectively, experimental peak fluences in this study only reached 1.59 J/cm^2. All other components showed no variation between the manufactured surface and laser-irradiated manufactured surface, therefore proving that high-intensity femtosecond laser pulses do not affect the silicate glass surface chemistry.

3.2 Surface hardness and densification

Both laser-irradiated and untreated glass surface indentation results are shown in Fig. 5. Untreated glass surface compositions have a standard deviation of ≤ 0.08 GPa. Post-treated surfaces observe a greater standard deviation; Borofloat and SLS approximately 0.11 GPa and ABS 0.18 GPa. Increased deviation in calculated surface hardness of laser exposed glasses is believed to result from a more highly disordered structure. High-intensity pulse irradiation will cause distortion to interatomic bond angles and lengths, therefore increasing surface hardness variability.

Vicker's hardness comparison before and after laser exposure is illustrated in Fig. 5. Under ambient conditions two of three silicate systems experienced an increase in surface hardness between 18.8 and 20.2%. SLS glass surface hardness was reduced by 16.6%. Polarized light microscopy confirmed that the hardening effect in BF and ABS glasses was not a result of generating stress fields. Sample stress was observed using a polarimeter (70 × 90 mm field, 0–140 nm retardation with orientation, and ~ 0.3 nm resolution), to ensure both surface and bulk stress remained constant throughout laser processing. Annealing low stress glasses increases the surface hardness 6–9%, at most [28]. Given the standard effect from annealing on surface hardness, it is likely not the mechanism responsible for such a significant increase. Reduction of SLS surface hardness is believed to stem from its high network modifier content; nearly twice ABS. Increased modifier content reduces tetrahedra and increases Q^x species, causing silica rings to depolymerize. Open structures may be more susceptible to undergo an increase to interatomic bonding lengths and angles.

The THz refractive index spectrum for SLS and ABS glass is shown in Fig. 5. The cutoff frequency occurs when the intensity falls below the noise floor, at which point the signal to noise ratio was too low to calculate accurate dielectric properties. In the case of SLS glass, pulsed laser irradiation was found to decrease the refractive index. At higher frequencies, the delta between laser-modified and pristine decreased by approximately 50%. Identical laser exposure conditions for ABS glass resulted in a refractive index increase of 0.012 compared to an unmodified region. The change in refractive index is consistent at higher frequencies, where $\Delta n = 0.011$. These findings are consistent with type I modifications in both SLS and ABS due to the fact that no localized stress fields were generated and because low pulse energies can produce either a positive or negative index change depending on the type of glass [11, 29, 30].

X-ray reflectometry (XRR) is a surface-sensitive X-ray scattering technique that determines material density, interface roughness, and layer thickness. Because of its

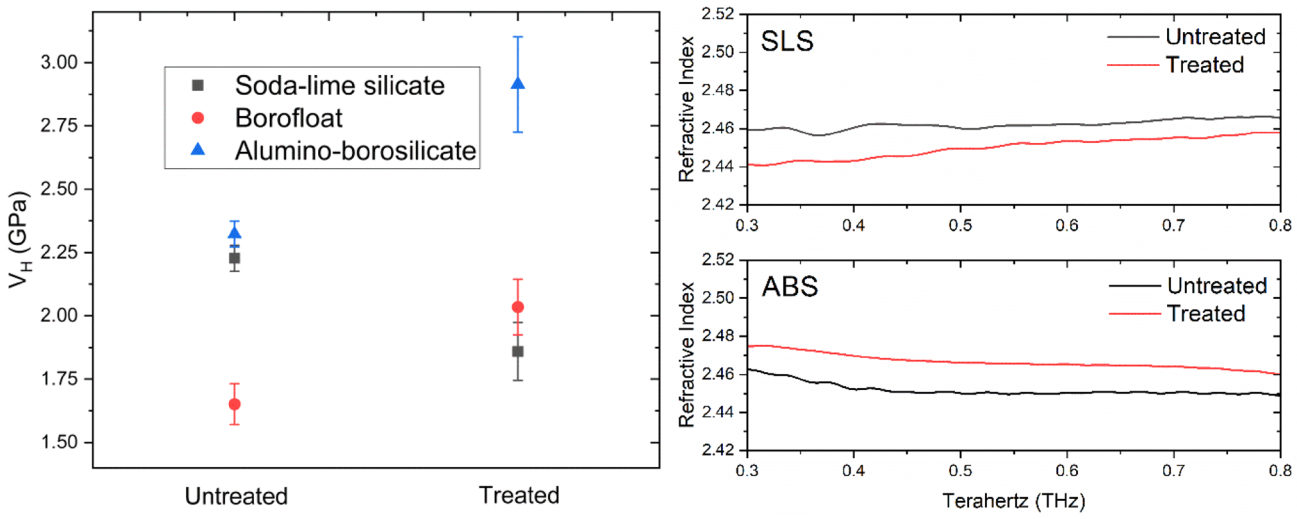

Fig. 5 Micro-indentation analysis of silicate glass surface hardness (left), refractive index as a function of frequency for soda-lime silicate and alumino-borosilicate

sensitivity to electron density, structural modification after laser exposure will be seen through X-ray scattering (although highly sensitive to roughness as it causes diffuse scattering, the interface roughness remained well below the standard 2–3 nm). Figure 6 shows the reflectivity pattern 2θ versus intensity of reflected X-ray photons. Pristine samples of both SLS and ABS glasses underwent density changes after laser exposure. The borosilicate observed increased scattering at higher 2θ and SLS scattering decreased at intermediate positions. Decreased scattering results in electron density reduction and vice versa. There is a high correlation between electron density and mass density in glass; increased electron density also increases refractive index. Interestingly, densification and decompaction do not occur at the same position. Decreased electron density in SLS begins around 0.75° 2θ, whereas the increase in ABS electron density begins at 1.5° 2θ. Interface roughness and densities are found in Table 2. These results validate our claim that femtosecond pulse irradiation induce structural changes in various silicate glasses.

Increasing angular ranging from 0.12° to 0.42° 2θ is a result of finite dimensions for a measured sample; this part of the pattern below the critical angle is not modeled. Below 0.12° the simultaneous effect of direct beam exposure and air scattering causes increasing intensity and has been ignored. Using a curve fitting procedure on the reflected profile, surface roughness and density are determined. Measured patterns were fitted by minimizing χ^2 through algorithmic refinement above the critical angle. ABS glass surface has undergone a densification of 5.2% after laser exposure while SLS surface density was reduced by 5.7%. The mechanism associated with the density changes is believed to be structural modification to interatomic bonds. As previously mentioned, reducing the bonding distance and angle on Si–O sites results in densification. Increasing these structural components causes decompaction and decrease in density [31].

Table 2 Silicate glass surfaces analyzed using X-ray reflectometry

Composition	Surface	Roughness (nm)	Profile	Density (g/cm^3)
ABS	Untreated	1.1946	No gradient	2.20
ABS	Treated	0.8288	No gradient	2.32
SLS	Untreated	1.314	No gradient	2.65
SLS	Treated	1.505	No gradient	2.50

4 Conclusion

In conclusion, we report surface hardening in various commercial silicate glasses. Femtosecond laser pulses have been shown to increase surface hardness in glasses with low modifier content 18.8–20.2% and decrease surface hardness of high-modifier content glasses by 16.6%. XPS and polarized microscopy validate the hardening mechanism operates without affecting surface chemistry or inducing residual stress layers within detectable limit of these tools. Scattering deviations in XRR characterization verify electron density deviations, therefore, supporting a change in near-surface density. Using a high-intensity femtosecond pulse laser, the surface hardness of glasses with variable modifier has shown contrasting effects. These results show promise for rapid strengthening of commercial glasses.

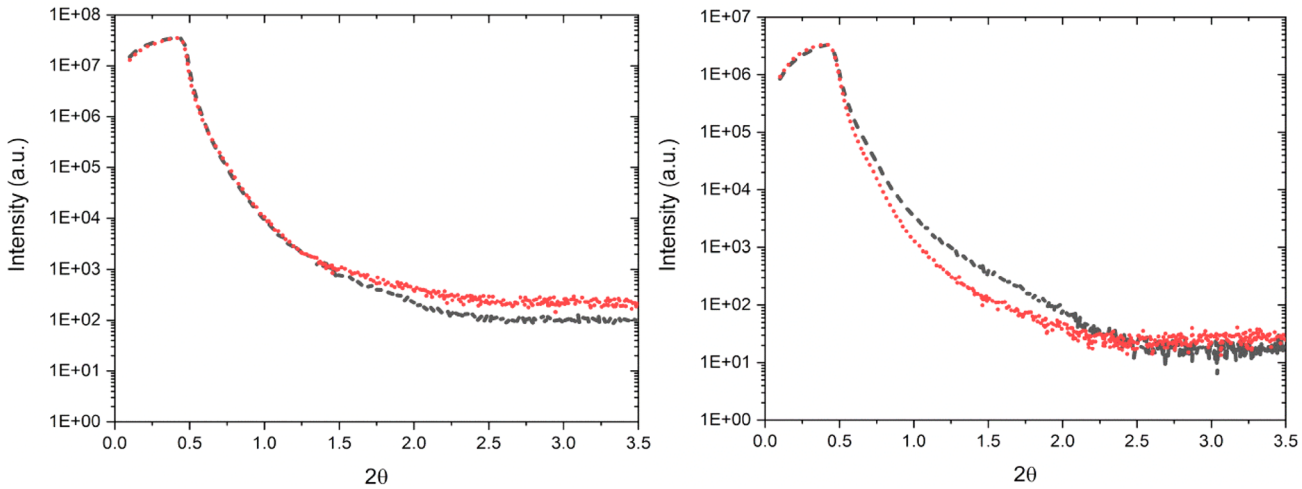

Fig. 6 X-ray reflectometry measurements before (black) and after (red) laser modification; left ABS, right SLS

References

1. D. Tan et al., Femtosecond laser induced phenomena in transparent solid materials: fundamentals and applications. Prog. Mater. Sci. **76**, 154–228 (2016)
2. K.M. Davis et al., Writing waveguides in glass with a femtosecond laser. Opt. Lett. **21**(21), 1729–1731 (1996)
3. R.R. Gattass, E. Mazur, Femtosecond laser micromachining in transparent materials. Nat. Photonics **2**(4), 219–225 (2008)
4. S. Kanehira, K. Miura, K. Hirao, Ion exchange in glass using femtosecond laser irradiation. Appl. Phys. Lett. **93**(2), 023112 (2008)
5. B. Poumellec et al., Modification thresholds in femtosecond laser processing of pure silica: review of dependencies on laser parameters [Invited]. Opt. Mater. Express **1**(4), 766–782 (2011)
6. B. Poumellec et al., Femtosecond laser irradiation stress induced in pure silica. Opt. Express **11**(9), 1070–1079 (2003)
7. C.B. Schaffer, *Interaction of Femtosecond Laser Pulses with Transparent Materials* (Diss. Harvard University, 2001)
8. A. Abou Khalil et al., Comparative study between the standard type I and the type A femtosecond laser induced refractive index change in silver containing glasses. Opt. Mater. Express **9**(6), 2640–2651 (2019)
9. D.J. Little et al., Mechanism of femtosecond-laser induced refractive index change in phosphate glass under a low repetition-rate regime. J. Appl. Phys. **108**(3), 033110 (2010)
10. C. D'Amico et al., Ultrafast laser-induced refractive index changes in Ge15As15S70 chalcogenide glass. Opt. Mater. Express **6**(6), 1914–1928 (2016)
11. S. Gross, M. Dubov, M.J. Withford, On the use of the type I and II scheme for classifying ultrafast laser direct-write photonics. Opt. Express **23**(6), 7767–7770 (2015)
12. V.R. Bhardwaj et al., Femtosecond laser-induced refractive index modification in multicomponent glasses. J. Appl. Phys. **97**(8), 083102 (2005)
13. D. Ehrt et al., Femtosecond-laser-writing in various glasses. J. Non-Cryst. Solids **345–346**, 332–337 (2004)
14. S.M. Eaton et al., Heat accumulation effects in femtosecond laser-written waveguides with variable repetition rate. Opt. Express **13**(12), 4708–4716 (2005)
15. T. Gorelik et al., Transmission electron microscopy studies of femtosecond laser induced modifications in quartz. Appl. Phys. A **76**(3), 309–311 (2003)
16. J.W. Chan et al., Structural changes in fused silica after exposure to focused femtosecond laser pulses. Opt. Lett. **26**(21), 1726–1728 (2001)
17. V.R. Bhardwaj et al., Stress in femtosecond-laser-written waveguides in fused silica. Opt. Lett. **29**(12), 1312–1314 (2004)
18. F. Luo et al., Redistribution of elements in glass induced by a high-repetition-rate femtosecond laser. Opt. Express **18**(6), 6262–6269 (2010)
19. M. Shimizu et al., Formation mechanism of element distribution in glass under femtosecond laser irradiation. Opt. Lett. **36**(11), 2161–2163 (2011)
20. T. Seuthe et al., in *Compositional Dependent Response of Silica-Based Glasses to Femtosecond Laser Pulse Irradiation*, vol 8885 (2013), p. 88850M
21. E. Mazur, Structural changes induced in transparent materials with ultrashort laser pulses. Ultrafast Lasers: Technol. Appl. **80**, 395 (2002)
22. V.P. Veiko et al., Femtosecond laser-induced stress-free ultra-densification inside porous glass. Laser Phys. Lett. **13**(5), 055901 (2016)
23. M. Douay et al., Densification involved in the UV-based photosensitivity of silica glasses and optical fibers: fiber gratings, photosensitivity, and poling. J. Lightwave Technol. **15**(8), 1329–1342 (1997)
24. J. Liu, Simple technique for measurements of pulsed Gaussian-beam spot sizes. Opt. Lett. **7**(5), 196–198 (1982)
25. R.G.C. Beerkens, Modeling the kinetics of volatilization from glass melts. J. Am. Ceram. Soc. **84**(9), 1952–1960 (2001)
26. H. Van Limpt, R. Beerkens, O. Verheijen, Models and experiments for sodium evaporation from sodium-containing silicate melts. J. Am. Ceram. Soc. **89**(11), 3446–3455 (2006)
27. N.P. Mellott, S. Brantley, C. Pantano, Topography of polished plates of albite crystal and glass during dissolution. Water Rock Interact. Ore Deposits Environ. Geochem. Tribute David A. Crerar **7**, 83–95 (2001)
28. M.M. Smedskjaer, M. Jensen, Y. Yue, Effect of thermal history and chemical composition on hardness of silicate glasses. J. Non-Cryst. Solids **356**(18), 893–897 (2010)
29. J. Petrovic, Durability of the refractive index change induced by a single femtosecond laser pulse in glass. Opt. Mater. X **1**, 100004 (2019)
30. A. Fuerbach, S. Gross, D. Little, A. Arriola, M. Ams, P. Dekker, M. Withford, Refractive index change mechanisms in different glasses induced by femtosecond laser irradiation. in *Pacific Rim Laser Damage 2016: Optical Materials for High Power Lasers*, vol. 9983 (Yokohama, Japan, 2016). https://doi.org/10.1117/12.2237368
31. K. Mishchik, *Ultrafast Laser-Induced Modification of Optical Glasses: A Spectroscopy Insight into the Microscopic Mechanisms* (Université Jean Monnet, Saint-Etienne, 2012)